RSC Advances

PAPER

View Article Online
View Journal | View Issue

Cite this: *RSC Adv.*, 2016, **6**, 2337

Elemental imaging of leaves from the metal hyperaccumulating plant *Noccaea caerulescens* shows different spatial distribution of Ni, Zn and Cd†

Damien L. Callahan,*[a] Dominic J. Hare,[b] David P. Bishop,[b] Philip A. Doble[b] and Ute Roessner[c]

Elemental imaging using laser ablation inductively coupled plasma mass spectrometry was performed on whole leaves of the hyperaccumulating plant *Noccaea caerulescens* after treatments with either Ni, Zn or Cd. These detailed elemental images reveal differences in the spatial distribution of these three elements across the leaf and provide new insights in the metal ion homeostasis within hyperaccumulating plants. In the Zn treated plants, Zn accumulated in the leaf tip while Mn was co-localised with Zn suggesting similar storage mechanisms for these two metals. These data show a Zn concentration difference of up to 13-fold higher in the distal part of the leaf. Also, there was no correlation between the S and Zn concentrations providing further evidence against S-binding ligands. In contrast, Ni was more evenly distributed while a more heterogeneous distribution of Cd was present with some high levels on leaf edges, suggesting that different storage and transport mechanisms are used for the hyperaccumulation of these two metals. These results show the importance of correct sampling when carrying out subcellular localisation studies as the hyperaccumulated elements are not necessarily homogenously distributed over the entire leaf area. The results also have great implications for biotechnological applications of *N. caerulescens* showing that it may be possible to use the mechanisms employed by *N. caerulescens* to increase the Zn concentration in nutrient poor crops without increasing the risk of accumulating other toxic elements such as Ni and Cd.

Received 13th November 2015
Accepted 19th December 2015

DOI: 10.1039/c5ra23953b

www.rsc.org/advances

Introduction

A disparate group of plants found in metal rich soils worldwide can accumulate extraordinary concentrations of metal ions or metalloids in their aerial tissues to concentrations which would be toxic to most other organisms. These plants are classified as *hyperaccumulators* and have developed unique mechanisms that enable the extreme accumulation of metal ions without suffering typical toxicity symptoms.[1] At high concentrations, the selectivity of transition elements to molecules containing nitrogen, oxygen and sulphur plus their access to different redox states result in extreme toxicity as the excess metal ions interfere with enzyme function and nitrogen metabolism, inhibit mitotic activities, cause oxidative damage and reduce the uptake of other essential micronutrients.[2–6] For these reasons, the transport, distribution and storage of these metallic micronutrients must be actively controlled. Over-accumulation of one metal ion can disrupt the overall metal ion homeostasis. There have been many studies which described the effects of heavy metal exposure in plants, for example, the review by Clemens contains an excellent description of these responses with a particular focus on Cd.[7]

Most hyperaccumulators have developed a tolerance for a particular metal ion and this tolerance is typically related to the soil substrate. The mechanisms behind this specificity and the detoxification mechanisms are not completely understood. Part of the challenge in studying hyperaccumulators is the great diversity in the types of plants which have these traits since they range from large rainforest trees such as *Pycnandra acuminata* (previously *Sebertia acuminata*) endemic to New Caledonia to small species belonging to the Brassicaceae family found throughout Europe.[1] For hyperaccumulation to occur the metal ions in above ground tissue must be sequestered and stored in subcellular structures in order to inhibit disruption of normal metabolic processes within the leaf.

[a]*Deakin University, School of Life and Environmental Sciences, Centre for Chemistry and Biotechnology, Burwood, Geelong, Victoria, 3125, Australia. E-mail: Damien.Callahan@deakin.edu.au*

[b]*Elemental Bio-imaging Facility, University of Technology Sydney, Australia*

[c]*Metabolomics Australia, School of BioSciences, The University of Melbourne, Parkville, Victoria, 3010, Australia*

† Electronic supplementary information (ESI) available. See DOI: 10.1039/c5ra23953b

Noccaea caerulescens (J & C Presl.) F. K. Mey. Brassicaceae (formerly *Thlaspi caerulescens*) has been identified as a model species for studying hyperaccumulation.[8,9] This species has the ability to hyperaccumulate Ni, Zn and Cd. Of note is that ecotypes from different metalliferous soils throughout Europe exhibit large variations in their accumulation abilities and tolerances for Ni, Zn or Cd.[10–13] An example of this is the Prayon ecotype which can accumulate more than 30 000 mg kg^{-1} Zn without showing any typical phenotypical responses of heavy metal toxicity such as chlorosis or reduced growth, however, it does not accumulate Cd to the same amounts as other ecotypes.[12,14]

Hyperaccumulating plants have considerable potential for remediation of contaminated soils through metal decontamination and re-establishment of vegetation cover. The potential applications of these plants have been recognised for some time and is one of the key drivers for research on these plants, therefore numerous reviews and books have been written for example the book by Chaney *et al.* nearly 20 years ago.[15] They also have great potential for biotechnological applications through the transfer of metal transport mechanisms into nutrient poor crops, known as biofortification. For review on the challenges of biofortification see Antosiewicz *et al.*[16]

In this study, laser ablation-inductively coupled plasma-mass spectrometry (LA-ICP-MS) was used to investigate the spatial distribution of the hyperaccumulated metal ions Ni^{2+}, Zn^{2+} and Cd^{2+} as well as other key micronutrients in whole *N. caerulescens* leaves from plants that had been treated with these metal ions individually. This imaging technique rasters a laser beam across samples and the ablated material is transported to the ICP-MS using an Ar carrier gas. The ICP-MS then detects ionised elements based on the mass-to-charge ratio. A particular strength of this technique is that multiple micronutrients may be measured in a single acquisition allowing the study of metal ion homeostasis and direct comparisons of micronutrient distribution in the same leaf. This technique has been used to study a broad range of matrices from geological samples to an array of different biological samples.[17,18] Although it does not have the fine spatial resolution of scanning electron microscopy or X-ray microanalysis, LA-ICP-MS is highly sensitive, has a large linear dynamic range as well as the ability for isotopic analysis. For a review of *in situ* elemental analysis in plants see Lombi *et al.*[19] There have been a number of studies using LA-ICP-MS on metal accumulation in plants, for example, it was used to coarsely map (750 μm^2) Ni in the roots from the Ni-hyperaccumulator *Berkheya coddii* Roessler, in leaves of *Helianthus annuus* (sunflower) with a spatial resolution of 200 μm, leaves from Cu treated *Elsholtzia splendens* leaves, Zn and Cu in roots of cucumber plants, boron in Poplar leaves and biofortification and localisation studies in wheat grains.[20–25] However, this is the first study that has spatially mapped metal ion distributions across whole leaves of a metal hyperaccumulating plant. This work reveals new information on the spatial distribution of hyperaccumulated metal ions and also illustrates the strength of this technique for studying micronutrients and metal ion homeostasis in plants.

Experimental

Plant growth and experimental design

Four different ecotypes of *N. caerulescens* were selected based on different reported abilities to hyperaccumulate Ni, Zn and Cd, they also represent populations from geographically distinct areas and soil types.[10–12,26] Seeds were germinated from populations in Bradford Dale (Derbyshire, U.K. – high capacity for Zn accumulation), Prayon (Belgium – high capacity of Zn accumulation, low Cd), Les Bleynard (Southern France – accumulate Zn and Cd) and Basadre (North Spain on Ni rich serpentine soil-expected high capacity to accumulate Ni and Zn) (Fig. 1).

Seeds were germinated and grown in Jiffy pots (sphagnum peat moss and wood pulp) in a glass house maintained at a maximum temperature of 22 °C with 14 hour day (supplemented with artificial grow lights) and 10 hour night. Plants were then watered with a 1/5 Hoagland's solution containing either $NiSO_4$ (250 μM), $ZnSO_4$ (500 μM) or $CdSO_4$ (10 μM) as well as a non-supplemented control group. These treatment concentrations allow normal growth of plants in relation to control and were selected based on a previous laboratory screening trial. Plants were treated one week after germination and were harvested after 3 months of growth. At least five individual replicate plants were grown from each ecotype in each of the four treatment regimes (control, Ni, Zn, Cd). The amounts which plants accumulate also depend on the growth conditions and bioavailability of metals supplied. In order to confirm the accumulation capabilities of the four selected ecotypes quantitative elemental analysis using an ICP-optical emission spectrometer (OES) was carried out on dried leaf tissues from these plants. The oldest leaf was selected for elemental imaging, while remaining leaves were immediately frozen in liquid nitrogen and stored at −80 °C. The leaves for imaging were washed with deionised water (18.2 MΩ) and methanol, placed between Whatman filter paper and stored under ambient conditions prior to imaging analysis. Minimal sample handling was undertaken in order to try and maintain metal ion distribution.

Total element concentrations

The total quantitative measurements were carried out from triplicate biological replicates. Approximately 100 mg fresh weight (FW) of the leaf tissue was taken from each plant, rinsed with deionised water (18.2 MΩ) and dried at 50 °C until a constant dry weight (DW) was observed. Dried and ground leaf material was accurately weighed (~15 mg) and acid digested at 70 °C for 3 hours in Eppendorf tubes (2.5 mL) with concentrated nitric acid (0.3 mL). The resulting clear acid digests were transferred to 10 mL volumetric flasks and made to volume with deionised water. Acid digest were analysed with a Varian Vista ICP-OES optical emission spectrometer (Varian Inc., Melbourne, Victoria, Australia) with the following settings: power 1 kW, plasma flow 15 L min^{-1}, auxiliary flow 1.5 L min^{-1} and nebuliser flow 0.9 L min^{-1}. Instrument data were evaluated using Vista Pro ICP expert 4.1.0. The instrument was calibrated

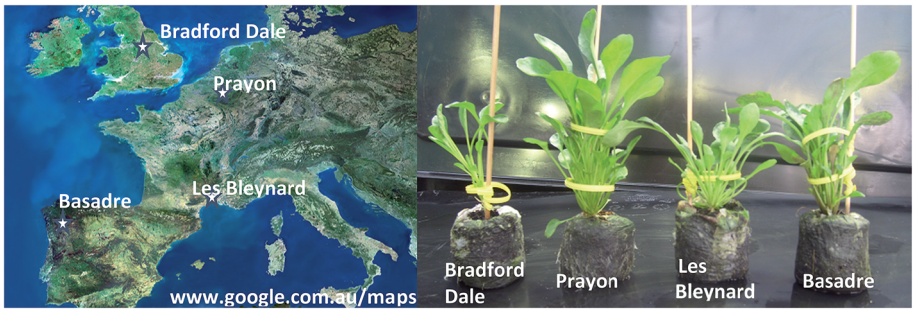

Fig. 1 (Left) Map showing the origin of seeds for each ecotype; (right) different ecotypes after three months growing in Jiffy Netted Pots (control group) showing clear morphological differences.

with standard solutions of Al, As, B, Cd, Cr, Cu, Fe, Hg, K, Pb, Co, Mn, Na, Ni, P, Se, V, Zn ranging between 5 mg L^{-1} and 100 mg L^{-1}. These solutions were prepared by appropriate dilutions with deionised water of the ICP mixed element stock standard (AM3, Choice Analytical, Australia) and B, K, Na, P (Choice Analytical, Australia) stocks.

Leaf sections were also made to quantitatively confirm the spatial distributions found by elemental imaging. The leaves that were snap frozen and stored were rinsed with de-ionised water then immediately sectioned into thirds (tip, middle, base). Each section was then placed into a separate pre-weighed 2 mL Eppendorf tube. This approach removes the chance for re-distribution of metal ions within the leaf tissues. Fresh weights and dry weights were recorded. The samples were then acid digested as above and elements quantified by ICP-MS (PerkinElmer NexION 350-X).

Laser ablation ICP-MS imaging

Samples were analysed using an Agilent 7500 ICP-MS (Agilent Technologies, Victoria, Australia) coupled to a New Wave Technologies UP-213 laser ablation system (Kennelec Technologies, Victoria, Australia). The laser ablation system contained a Nd:YAG laser and a large format laser ablation cell of 15.2 × 15.2 cm. The cell employed a roving sample cup which moved the stage in *x*–*y*–*z* directions while the laser beam position remained fixed. Tygon tubing (3 mm i.d.) transferred ablated ions using a stream of argon to the ICP-MS. The ICP-MS was tuned prior to each analysis using the NIST standard reference material 612, trace elements in glass. The following settings were used for the ICP-MS: RF power 1250 W, plasma gas flow rate 15 L min^{-1}, measured mass to charge ratios (*m*/*z*): C (*m*/*z* 13), Cd (*m*/*z* 111), Cu (*m*/*z* 63), Fe (*m*/*z* 57), K (*m*/*z* 39), Mg (*m*/*z* 24), Mn (*m*/*z* 55), Mo (*m*/*z* 95), Na (*m*/*z* 23), Ni (*m*/*z* 60), P (*m*/*z* 31), S (*m*/*z* 34), Zn (*m*/*z* 66). The laser was operated at 213 nm, repetition frequency 20 Hz, laser energy 30% power, resolution 80 μm, scan rate 99 μm s^{-1}. Approximately 150 lines per leaf were analysed producing a total run time of 15 hours per leaf. Leaves were ablated from the top leaf surface.

Each scan line produces a (.csv) file, which was collated using a Visual Basic macro (Microsoft) and imported into ENVI (Exelis, Boulder, Co., USA) for image analysis.[27]

Results and discussion

Total element concentration

Correlating to previous studies, the unique ecotypes accumulated different concentrations of each metal ion (Fig. 2) even though they were grown side by side and treated with the same solutions. The variation in accumulation capabilities of the different ecotypes provides a rich area for research but was not the main focus of this study. The Prayon ecotype accumulated approximately twice the concentration of Zn (7900 mg kg^{-1} dw) in comparison to the next highest ecotype from Le Bleynard in Southern France (4020 mg kg^{-1} dw). Although Prayon plants accumulated the highest Zn concentrations they accumulated approximately 10-fold less of the other two metal treatments, Ni and Cd. This low accumulation factor for the Prayon population has been observed previously.[26] The Puente Basadre ecotype accumulated the highest Cd concentration (960 mg kg^{-1} dw) while the Bradford Dale and Le Blaynard had the highest Ni concentrations (740 mg kg^{-1}, 720 mg kg^{-1} respectively). As expected all treated plants had significantly more of the added metal ion then the non-treated controls (ESI Fig. S1†). The

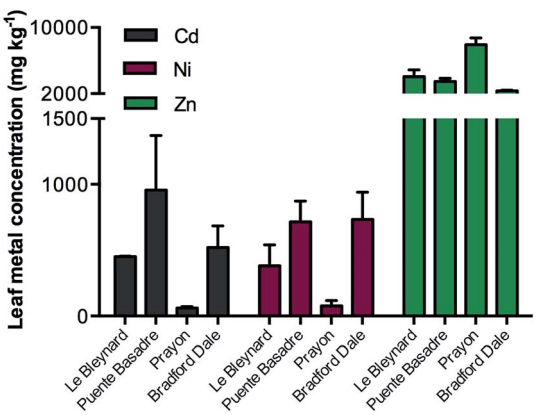

Fig. 2 Total Ni, Zn and Cd elemental concentrations in leaf tissues from treated plants of the four different ecotypes grown. Bars are grouped by the three treatments either $CdSO_4$ (10 μM; black), $NiSO_4$ (250 μM; red), $ZnSO_4$ (500 μM; green). Control plant values omitted from this graph due to comparatively low concentrations of these elements. Full elemental values in Online Resource 1.

Puente Basadre ecotype was selected for subsequent elemental images as it contained the high levels of all three treated metal ions. A sample of the Prayon ecotype was also imaged to determine if there were any differences between ecotypes with regards to elemental distributions.

Elemental images

N. caerulescens has the ability to accumulate up to 3% Zn in its dry mass and therefore could exceed the maximum signal intensity of the instrumentation. This would provide a non-linear response to Zn due to saturation of the detector signal. To determine the maximum concentration range of the LA-ICP-MS system, dried, ground tissues from hydroponically grown *N. caerulescens* plants grown in a previous study were pressed into a disk.[28] These represented tissue concentrations at 300, 11 000, 15 000 and 20 000 mg kg^{-1} leaf dry mass.[28] The ICP-MS signal was saturated between the 11 000–15 000 mg kg^{-1} samples. The samples analysed in this study were well below this threshold and therefore represent images within the linear dynamic range of the instrument.

Images based on the elemental intensity were produced for each measured element and are represented here either normalised to the ^{13}C isotope or plotted based on the raw signal intensity. The fine resolution of these images show obvious features in the leaves, in particular leaf venation (Fig. 3–5). A striking accumulation pattern was observed from the Zn-treated plants (Fig. 3). Significantly higher concentrations of Zn were clearly identified in the leaf tip. A Zn concentration gradient is present from the leaf tip to approximately half way down the lamina. The relative differences in elemental concentrations were determined using the mean signal intensity from key spatial regions of the leaf. For the Zn image, this represents a 13-fold higher concentration of Zn at the leaf tip compared to the base of the leaf (Fig. 3). The bottom half of the lamina (closest to the petiole) contained a relatively homogenous Zn concentration. The Zn-concentration supplied to the plants was

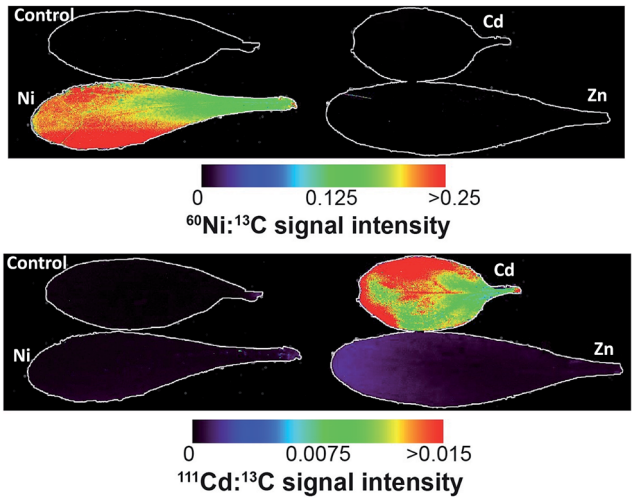

Fig. 4 Ni (top) and Cd (bottom) images from the different treatments from the Puente Basadre population. The Ni elemental image shows a relatively homogenous distribution, while Cd shows a more heterogeneous distribution with some increased Cd concentration on the leaf edges. Note in the signal intensity from the plants not treated with the corresponding metal are outlined due to the low relative intensity. Non-normalised images are in ESI.†

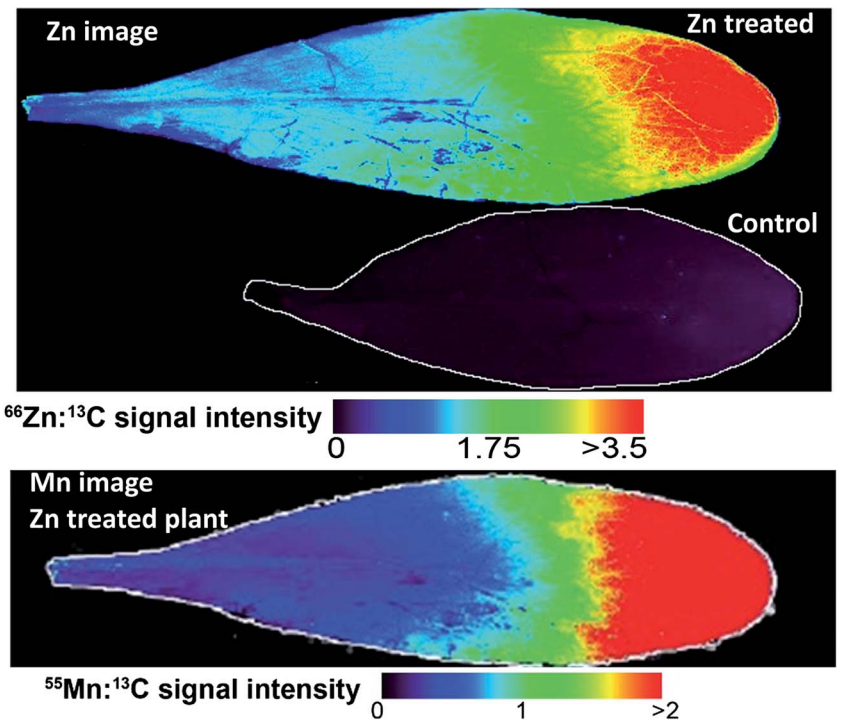

Fig. 3 Elemental images from the Puente Basadre population. Top, Zn heatmap showing distribution in leaves from a Zn treated plant and control plant (outlined due to low relative signal). Zn intensity was normalised using the ^{13}C signal. Bottom panel showing a similar distribution for Mn.

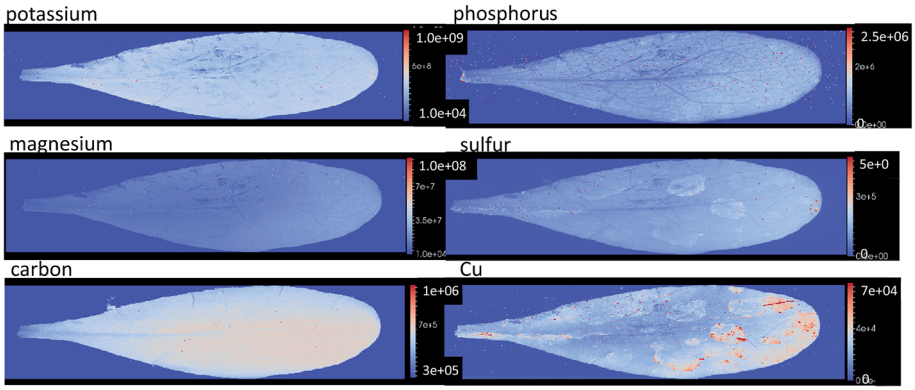

Fig. 5 Elemental images based on the raw signal intensity of potassium, phosphorous, magnesium, sulfur, carbon, and copper from Zn treated plant showing a homogenous distribution of these macro elements. The intensity values of these images illustrated on the bar to the right of each image. Not some contamination of leaf surface can be seen in the copper image. All images available in ESI 4.†

constant throughout the 3 month growth period and therefore the plant is actively concentrating Zn at the leaf tip. It is also clear from these images that Zn was lower in concentration in the vascular tissues, where the leaf veins are darker and therefore lower in Zn-concentration. The Zn treated Prayon ecotype was also imaged had the same Zn-accumulation pattern as the Puente Basadre ecotype suggesting similar storage mechanisms for Zn (ESI Fig. S2†). Examination of other images showed a very clear co-localisation of Mn and Zn (Fig. 3). From previous work in our laboratory, a clear reduction in Mn was observed when the plant Zn concentration exceeded 10 000 mg kg^{-1} (ESI Fig. S3†).[28] This suggests that Zn and Mn have similar uptake mechanisms and also explains why the Mn concentration decreases when *N. caerulescens* accumulates extremely high concentrations of Zn. No other elements showed the same striking co-localisation patterns in the Zn-treated plants. Sulphur showed some increase in intensity (2-fold difference) at the leaf tip but not to the same extent of Zn providing further evidence against S-binding ligands as part of storage in *N. caerulescens*.[29] The Zn image of the non-treated control leaf on the same scale of the treated plants is hardly discernible (Fig. 3).

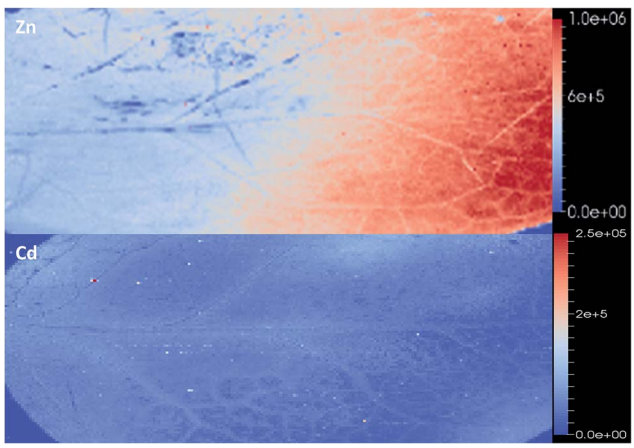

Fig. 6 Zoomed in image of Zn (top) and Cd (bottom). Higher Zn concentrations are located outside the vascular tissue in contrast to Cd. Images are produced on the raw signal intensity.

However, in the leaf from a control plant, which has a 3.5-fold lower total leaf Zn concentration, a similar accumulation pattern was observed with higher concentrations in the leaf tip (2-fold). No other accumulation patterns were observed for the other elements in the control plants (ESI Fig. S4†). From the Fe and Cu images it appears that some leaf contamination occurred which was not removed by washing. This most likely occurred during the supply of nutrient solutions to the plants causing the precipitation of insoluble Fe and Cu salts on the leaf surface (Fig. 5, ESI Fig S4†). However it can still be observed in the Fe and Cu images that concentrations of these elements are not effected by high localised concentrations of Zn. The same homogenous distribution is also observed in leaves from plants treated with Ni and Cd.

As expected the elemental images from the Ni and Cd treated plants show a huge contrast in signal intensities relative to the non-treated plants (Fig. 4). The elemental images in the Ni and Cd treated plants did not show any distinct accumulation patterns. Ni was relatively evenly distributed across the whole leaf with lower concentrations in leaf vascular tissue (Fig. 4). No clear pattern could be observed for Cd distribution apart from having higher concentrations in leaf vascular tissue and some of the leaf edges (Fig. 5 and 6). The more heterogeneous Cd distribution is in contrast to Zn and Ni. These images reveal that even though multiple elements are hyperaccumulated by *N. caerulescens*, different storage strategies are used for Ni, Zn and Cd. It is evident that in *N. caerulescens* Zn accumulation begins at the distal part of the lamina. In contrast, there is no regional concentration for Ni. A closer examination of the Cd and Cu images show higher concentrations in the vascular tissues of the lamina in comparison to surrounding tissue which also contrasts to Zn and Ni. This is most apparent in the zoomed in elemental images of Zn *versus* Cd (Fig. 6). As discussed above the elemental imaging technique used here cannot produce images which would enable conclusions to be made at the subcellular level. Molecular studies have shown that Zn is transported symplastically by various highly expressed membrane transporters such as the HMA4 (Heavy Metal ATPase 4) and ZIP (Zn regulated transporter, iron-regulated transporter-

Table 1 Quantitative confirmation of elemental distributions found by elemental imaging. Results are from plants treated with either Ni, Zn or Cd. The leaves were sectioned into thirds; base, middle and tip, dried, acid digested and analysed by ICP-MS

	Base	Mid	Tip
Zn (mg kg^{-1}) dw			
Zn-1	420	1400	1700
Zn-2	239	600	1200
Zn-3	150	640	1600
Zn-4	1500	3700	6500
Ni (mg kg^{-1}) dw			
Ni-1	370	550	630
Ni-2	590	700	960
Ni-3	410	1900	1300
Cd (mg kg^{-1}) dw			
Cd-1	210	370	340
Cd-2	150	300	380
Cd-3	190	220	230

related protein) gene families.[32,33] With regards to Cd there is no solid evidence for apoplastic localisation of Cd in leaves. A very early study which claimed apoplastic storage was most likely due to sample preparation artefact due to the chemical fixation technique used.[30] It was subsequently shown that Cd is actively taken up into the epidermal storage cells.[31,34]

The distribution of macro elements such as Na, K, Mg, S and Fe show a homogenous distribution throughout the leaves in all treatments. This shows that the concentrations of these key elements are not affected by the presence of high concentrations of the hyperaccumulated metal ion (Fig. 5).

As the imaging data showed differences elemental spatial distributions, quantitative measurements were made to confirm that the patterns observed were not an artefact of sample preparation. These quantitative measurements were also carried out in triplicate to provide replication of these observations. The leaves were sectioned into thirds: tip, middle and base, oven dried, acid digested then total elemental concentrations determined by solution ICP-MS. These measurements confirm the elemental imaging data (Table 1) with 4–10 fold higher concentrations of Zn in the leaf tip and more homogenous distributions of Ni and Cd.

Only a few published studies to date have examined the macro leaf spatial distribution of elements in hyperaccumulators. One study analysed leaf cross sections using micro-PIXE and found a homogenous distribution of Ni in different cell types in the Australian Ni hyperaccumulator *Stackhousia tryonii*, suggesting that a similar accumulation pattern was observed to this study.[35] The radioactive ^{109}Cd isotope was used previously to image Cd compartmentation at the leaf scale in the hyperaccumulators *N. caerulescens*, *Arabidopsis halleri* and willow leaves.[36–38] These studies agree with the results described here. In the three species referenced the authors showed a heterogeneous Cd distribution in the older leaves, in particular, high concentrations in vascular tissues and leaf edges. The paper by Cosio *et al.* (2005) is of particular relevance to this work. The Cd autoradiography was carried out on two contrasting ecotypes of *N. caerulescens*. This work clearly showed Cd localised at leaf edges as well as points of higher concentration spread out over the whole leaf surface. X-ray microanalysis of the Cd cellular distribution showed that Cd was stored in less metabolically active areas of leaf cells. Unfortunately this study did not carry out a similar analysis for Zn. An early study comparing Cd and Zn uptake also showed different distribution patterns for these metals based on leaf age.[39] The study by Perronnet *et al.* (2003) showed that Cd concentrations remained relatively constant with increasing biomass while Zn concentrations had a small decrease with time. It has also been shown that Cd is not re-distributed from old to young organs during leaf senescence suggesting that Cd ions are fixed in place once accumulated.[40] This is in contrast to Zn which is actively take up and concentrated in leaf tissues by *N. caerulescens*.[41] Other studies have shown that the Cd co-ordination environment changes with tissue age. For example, tissue age differences in the concentration and the co-ordination environment of Cd were observed *N. caerulescens* leaf tissue using X-ray absorption spectroscopy.[42]

The determination of the spatial distribution of elements is important for understanding how hyperaccumulators transport and store the large amounts of metals in a way that does not interfere with essential metabolic processes and maintains elemental homeostasis. The findings here also have implications for tissue sampling. For example, a recent study focussed on trace elements in hyperaccumulators from New Caledonia, it was shown concentrations of Mn increase in the older leaves of the hyperaccumulator *Grevillea meisneri*.[43] These findings illustrate the importance of correct sampling and the consideration of leaf age when determining the ability and the mechanisms of plants to accumulate trace elements.

Most research on metal ion distribution in hyperaccumulators has focused on cellular and sub-cellular distributions as opposed to whole tissues as was carried out in this research. For a review on elemental distribution in plants see Zhao *et al.* 2014.[44] There have been some conflicting reports of the cellular metal ion distribution in *N. caerulescens* and other closely related species using X-ray microanalysis techniques. For example, organelle isolation found that 65–70% of the total leaf Cd and Zn was located in vacuoles of mesophyll tissues in *N. caerulescens*.[45] However, other studies have shown Zn storage in the epidermis cells instead of the metabolically active mesophyll layer.[46–48] The conflict here may be due to different sample preparation techniques. The paper by Ma *et al.* (2005) removed the epidermal layer.[45] This may have resulted in the rupture of epidermal cells with the cell contents transferring to the mesophyll layer.

Here we have shown the importance of selecting the correct areas within the leaf to study subcellular localisation and to first confirm if there is a difference on the spatial distribution of elements. A single leaf cross section may not represent the same distribution across the whole leaf. The spatial resolution of the LA-ICP-MS does not allow imaging of subcellular structures, however it is highly sensitive and whole leaf elemental images still provide useful information on the metal-ion homeostasis in plants.

Conclusions

The large variation observed in the total elemental concentrations of the four ecotypes illustrates the rich diversity present in the *N. caerulescens* hyperaccumulator. The use of LA-ICP-MS has allowed multiple elemental images to be developed without the use of radioactive labelling and with minimal sample preparation, however, the analysis itself is destructive. This technique is highly sensitive and has a large dynamic range that enables measurements of trace elements as well as hyperaccumulated metals in plants. In this study it was revealed that Zn accumulates distal area within the leaf and co-localises with Mn and to some degree S. No other elements showed co-localisation with Zn. In contrast to Zn, Ni is more homogenously distributed across the leaf while a more un-even distribution of Cd was found, with clearly higher concentrations in vascular tissues. These results show the importance of correct sampling when studying hyperaccumulators as the hyperaccumulated elements may not be distributed evenly across a leaf and therefore subcellular studies must take this into account.

Finally, as Zn is stored differently to Ni, and Cd it may be possible to utilise the selectivity of the Zn transporters used by *N. caerulescens* in future biofortification studies without the risk of increasing Ni and Cd concentrations.

Acknowledgements

This research was supported by funding from Deakin University and the central research grants scheme (CRGS) and an early career researcher grant from The University of Melbourne. DL Callahan would like to thank Vasalisa Pendan for help with plant growth. The authors would also like to thank Prof. Alan Baker for provision of the *N. caerulescens* seed bank.

References

1 U. Krämer, *Annu. Rev. Plant Biol.*, 2010, **61**, 517–534.
2 C. Anderson, A. Deram, D. Petit, R. Brooks, R. Stewart and R. Simcock, in *Trace Elements in Soil: Bioavailability, Flux, and Transfer*, ed. I. K. Iskandar and M. B. Kirkham, CRC Press, Boca Raton, 2001, ch. 4, pp. 63–76.
3 C. Chen, D. Huang and J. Liu, *Clean: Soil, Air, Water*, 2009, **37**, 304–313.
4 E. Gajewska, M. Wielanek, K. Bergier and M. Skłodowska, *Acta Physiol. Plant.*, 2009, **31**, 1291–1300.
5 K. V. Madhava Rao and T. V. S. Sresty, *Plant Sci.*, 2000, **157**, 113–128.
6 J. Molas, *Environ. Exp. Bot.*, 2002, **47**, 115–126.
7 S. Clemens, *Biochimie*, 2006, **88**, 1707–1719.
8 A. G. L. Assunção, H. Schat and M. G. M. Aarts, *New Phytol.*, 2003, **159**, 351–360.
9 M. J. Milner and L. V. Kochian, *Ann. Bot.*, 2008, **102**, 3–13.
10 A. Baker, R. Reeves and A. Hajar, *New Phytol.*, 1994, **127**, 61–68.
11 R. D. Reeves, C. Schwartz, J. L. Morel and J. Edmondson, *Int. J. Phytorem.*, 2001, **3**, 145–172.
12 E. Lombi, F. J. Zhao, S. J. Dunham and S. P. McGrath, *New Phytol.*, 2000, **145**, 11–20.
13 A. G. L. Assunção, W. M. Bookum, H. J. M. Nelissen, R. Vooijs, H. Schat and W. H. O. Ernst, *New Phytol.*, 2003, **159**, 411–419.
14 S. L. Brown, R. L. Chaney, J. S. Angle and A. J. M. Baker, *Soil Sci. Soc. Am. J.*, 1995, **59**, 125.
15 R. L. Chaney, M. Malik, Y. M. Li, S. L. Brown, E. P. Brewer, J. S. Angle and A. J. Baker, *Curr. Opin. Biotechnol.*, 1997, **8**, 279–284.
16 D. M. Antosiewicz, A. Barabasz and O. Siemianowski, *Front. Plant Sci.*, 2014, **5**, 80.
17 J. S. Becker, M. Zoriy, A. Matusch, B. Wu, D. Salber, C. Palm and J. S. Becker, *Mass Spectrom. Rev.*, 2010, **29**, 156–175.
18 D. Pozebon, G. L. Scheffler, V. L. Dressler and M. A. G. Nunes, *J. Anal. At. Spectrom.*, 2014, **29**, 2204–2228.
19 E. Lombi, K. G. Scheckel and I. M. Kempson, *Environ. Exp. Bot.*, 2011, **72**, 3–17.
20 A. B. Moradi, S. Swoboda, B. Robinson, T. Prohaska, A. Kaestner, S. E. Oswald, W. W. Wenzel and R. Schulin, *Environ. Exp. Bot.*, 2010, **69**, 24–31.
21 B. Wu, M. Zoriy, Y. Chen and J. S. Becker, *Talanta*, 2009, **78**, 132–137.
22 J. Shi, M. A. Gras and W. K. Silk, *Planta*, 2009, **229**, 945–954.
23 R. Rees, B. H. Robinson, M. Menon, E. Lehmann, M. S. Gunthardt-Goerg and R. Schulin, *Environ. Sci. Technol.*, 2011, **45**, 10538–10543.
24 I. Cakmak, M. Kalayci, Y. Kaya, A. A. Torun, N. Aydin, Y. Wang, Z. Arisoy, H. Erdem, A. Yazici, O. Gokmen, L. Ozturk and W. J. Horst, *J. Agric. Food Chem.*, 2010, **58**, 9092–9102.
25 B. Wu, F. Andersch, W. Weschke, H. Weber and J. S. Becker, *Metallomics*, 2013, **5**, 1276–1284.
26 N. Roosens, N. Verbruggen, P. Meerts, P. Ximenez-Embun and J. A. C. Smith, *Plant, Cell Environ.*, 2003, **26**, 1657–1672.
27 D. Hare, B. Reedy, R. Grimm, S. Wilkins, I. Volitakis, J. L. George, R. A. Cherny, A. I. Bush, D. I. Finkelstein and P. Doble, *Metallomics*, 2009, **1**, 53–58.
28 S. Foroughi, A. J. M. Baker, U. Roessner, A. A. T. Johnson, A. Bacic and D. L. Callahan, *Metallomics*, 2014, **6**, 1671–1682.
29 V. H. Hassinen, M. Tuomainen, S. Peräniemi, H. Schat, S. O. Kärenlampi and A. I. Tervahauta, *J. Exp. Bot.*, 2009, **60**, 187–196.
30 M. D. Vázquez, J. Barceló, C. Poschenrieder, J. Mádico, P. Hatton, A. J. M. Baker and G. H. Cope, *J. Plant Physiol.*, 1992, **140**, 350–355.
31 M. Wójcik, J. Vangronsveld, J. D'Haen and A. Tukiendorf, *Environ. Exp. Bot.*, 2005, **53**, 163–171.
32 A. Assunção, P. Martins, S. de Folter, R. Vooijs, H. Schat and M. Aarts, *Plant, Cell Environ.*, 2001, **24**, 217–226.
33 N. S. Pence, P. B. Larsen, S. D. Ebbs, D. L. Letham, M. M. Lasat, D. F. Garvin, D. Eide and L. V. Kochian, *Proc. Natl. Acad. Sci. U. S. A.*, 2000, **97**, 4956–4960.
34 B. Leitenmaier and H. Kupper, *Plant, Cell Environ.*, 2011, **34**, 208–219.
35 N. P. Bhatia, K. B. Walsh, I. Orlic, R. Siegele, N. Ashwath and A. J. M. Baker, *Funct. Plant Biol.*, 2004, **31**, 1061–1074.

36 C. Cosio, L. DeSantis, B. Frey, S. Diallo and C. Keller, *J. Exp. Bot.*, 2005, **56**, 765–775.
37 C. Cosio, P. Vollenweider and C. Keller, *Environ. Exp. Bot.*, 2006, **58**, 64–74.
38 S. Huguet, V. Bert, A. Laboudigue, V. Barthès, M.-P. Isaure, I. Llorens, H. Schat and G. Sarret, *Environ. Exp. Bot.*, 2012, **82**, 54–65.
39 K. Perronnet, C. Schwartz and J. Morel, *Plant Soil*, 2003, **249**, 19–25.
40 L. Lovy, D. Latt and T. Sterckeman, *Plant Soil*, 2013, **362**, 345–354.
41 S. N. Whiting, J. R. Leake, S. P. McGrath and A. J. M. Baker, *New Phytol.*, 2000, **145**, 199–210.
42 H. Küpper, A. Mijovilovich, W. Meyer-Klaucke and P. M. H. Kroneck, *Plant Physiol.*, 2004, **134**, 748–757.
43 G. Losfeld, L. L'Huillier, B. Fogliani, S. Coy, C. Grison and T. Jaffré, *Environ. Sci. Pollut. Res.*, 2015, **22**, 5620–5632.
44 F.-J. Zhao, K. L. Moore, E. Lombi and Y.-G. Zhu, *Trends Plant Sci.*, 2014, **19**, 183–192.
45 J. F. Ma, D. Ueno, F.-J. Zhao and S. P. McGrath, *Planta*, 2005, **220**, 731–736.
46 U. Krämer, I. J. Pickering, R. C. Prince, I. Raskin and D. E. Salt, *Plant Physiol.*, 2000, **122**, 1343–1353.
47 H. Küpper, F. Jie Zhao and S. P. McGrath, *Plant Physiol.*, 1999, **119**, 305–312.
48 K. Vogel-Mikus, J. Simcic, P. Pelicon, M. Budnar, P. Kump, M. Necemer, J. Mesjasz-Przybylowicz, W. J. Przybylowicz and M. Regvar, *Plant, Cell Environ.*, 2008, **31**, 1484–1496.